

## KEPLER AND THE KUIPER BELT

B. SCOTT GAUDI

Harvard-Smithsonian Center for Astrophysics, 60 Garden St., Cambridge, MA 02138  
Draft version October 3, 2018

### ABSTRACT

The proposed field-of-view of the *Kepler* mission is at an ecliptic latitude of  $\sim 55^\circ$ , where the surface density of scattered Kuiper Belt Objects (KBOs) is a few percent that in the ecliptic plane. The rate of occultations of *Kepler* target stars by scattered KBOs with radii  $r \gtrsim 10$  km is  $\sim 10^{-6} - 10^{-4}$  star<sup>-1</sup> yr<sup>-1</sup>, where the uncertainty reflects the current ignorance of the thickness of the scattered KBO disk and the faint-end slope of their magnitude distribution. These occultation events will last only  $\sim 0.1\%$  of the planned  $t_{\text{exp}} = 15$  minute integration time, and thus will appear as single data points that deviate by tiny amounts. However, given the target photometric accuracy of *Kepler*, these deviations will nevertheless be highly significant, with typical signal-to-noise ratios of  $\sim 10$ . I estimate that  $\sim 1 - 20$  of the  $10^5$  main-sequence stars in *Kepler*'s field-of-view will exhibit detectable occultations during its four-year mission. For unresolved events, the signal-to-noise of individual occultations scales as  $t_{\text{exp}}^{-1/2}$ , and the minimum detectable radius could be decreased by an order of magnitude to  $\sim 1$  km by searching the individual 3 sec readouts for occultations. I propose a number of methods by which occultation events may be differentiated from systematic effects. *Kepler* should measure or significantly constrain the frequency of highly-inclined,  $\sim 10$  km-sized KBOs.

*Subject headings:* Kuiper Belt – occultations – solar system: formation – techniques: photometric

### 1. INTRODUCTION

The Kuiper belt (see Luu & Jewitt 2002 for a review) constitutes one of the few fossil records of the formation of planets and planetesimals in the early solar system. It is therefore of great interest to determine the ensemble properties of its denizens. These properties provide clues to the physical processes operating in the protoplanetary solar disk, as well as in the subsequent evolution of the solar system.

Kuiper Belt Objects (KBOs) are currently discovered in deep optical imaging surveys that are primarily limited to latitudes within  $\sim 10^\circ$  of the ecliptic or invariable plane (see, e.g., Millis et al. 2002). The apparent  $R$ -magnitude of a KBO at a distance of  $a \simeq 40$  AU with radius  $r \simeq 100$  km is  $m_R \simeq 23.4$ , assuming an albedo of 4%. Since the flux of a KBO arises from reflected sunlight, it is proportional to  $r^2$  and  $a^{-4}$ . Therefore, imaging surveys are only able to detect relatively large and nearby KBOs with reasonable expenditure of resources. Furthermore, in order to have the best chance of success, they do not target high ecliptic latitudes, and are therefore biased against KBOs with large inclinations  $i$ .

Large KBOs are known to fall into at least three dynamical classes. Classical KBOs are relatively dynamically cold, with eccentricities  $e \lesssim 0.3$  and  $i \lesssim 5^\circ$ . Resonant KBOs are in mean motion resonances with Neptune, and were likely trapped there and subsequently excited to high  $i$  and  $e$  by the outward migration of Neptune (Malhotra 1995). Scattered KBOs have very broad  $e$  and  $i$  distributions, and have probably been excited by some as-yet unknown process.

The size distribution of large KBOs is known to follow the form of  $r^{-q}$ , with  $q \simeq 4$ , and a surface density of objects of  $1 \text{ deg}^{-2}$  at  $r \simeq 100$  km. For  $r \lesssim 100$  km, collisions will preferentially destroy KBOs, so that below a certain radius  $r < r_b \lesssim 100$  km, the size distribution is expected to flatten. This break radius is set by the

dynamical and physical properties of the KBOs, and is roughly where the collision time is equal to the age of the system. The first estimate of this break radius, based on deep Hubble Space Telescope (HST) observations, yields  $r_b \sim 70$  km (Bernstein et al. 2004, hereafter B04).

Unfortunately, it will be difficult, in the near future, to learn about the properties of small KBOs beyond what is already known using direct imaging, and especially so for those with high inclinations. Further progress will require next-generation synoptic surveys (Pan-STARRS, Kaiser et al. 2002; The Discovery Channel Telescope, Millis, Dunham, & Sebring 2003; LSST, Tyson 2002), or new methods. One such method, first proposed by Bailey (1976), is to search for stellar occultations by foreground KBOs. This technique has been explored by several authors (Brown & Webster 1997; Cooray & Farmer 2003; Dyson 1992), and is being implemented by Roques et al. (2003), and the Taiwanese-American Occultation Survey (TAOS; Liang et al. 2003). However, due to the low expected event rate, the first occultation surveys will likely focus on low-latitude fields. Therefore, the statistics of small, high-inclination KBOs will remain meager.

Here I explore the possibility of measuring the surface density of small KBOs with high inclinations using the NASA space mission *Kepler*. *Kepler*'s main goal is to detect transiting planets around normal stars, and it is far from ideally suited to detect occultations by foreground KBOs, especially given the high latitude ( $55^\circ$ ) of its target field, and its long (15 min) exposure time. However, due to the large number of target stars and extraordinary photometric precision, I demonstrate that it may nonetheless detect a significant number of occultation events. If these can be separated from systematic artifacts, *Kepler* should be able to determine or severely constrain the frequency of small, high-inclination KBOs.

## 2. ORDER-OF-MAGNITUDE ESTIMATES

I begin by providing order-of-magnitude estimates of the rate and properties of KBO occultation events in *Kepler's* field-of-view (FOV). Assuming all KBOs are at the same distance, the optical depth to occultations is roughly the differential angular surface density  $\Sigma_r(r) = dN(r)/drd\Omega$  of KBOs of radius  $r$  in the *Kepler* FOV, times the solid angle  $\Omega(r)$  subtended by a KBO of radius  $r$ , integrated over all radii,

$$\tau \sim \int dr \Omega(r) \Sigma_r(r). \quad (1)$$

Although the optical depth to KBOs at a constant distance is most directly related to their size distribution, optical surveys do not directly constrain this quantity. Rather, they constrain the distribution of apparent magnitudes. I therefore switch the integration variable in equation (1) to apparent  $R$ -magnitude  $m_R$ ,

$$\tau \sim \int dm_R \Omega(m_R) \Sigma(m_R). \quad (2)$$

Assuming constant albedo and distance, the radius of a KBO is related to its  $R$ -magnitude by

$$r(m_R) = r_{23} 10^{-0.2(m_R-23)}. \quad (3)$$

where  $r_{23}$  is the radius of a KBO at  $m_R = 23$ . The measured differential surface density  $\Sigma(r) = dN(r)/dm_R d\Omega$  of all bright KBOs as a function of apparent magnitude near the ecliptic has the form  $\Sigma(m_R) = \Sigma_{23} 10^{\alpha(m_R-23)}$ , where  $\alpha$  can be related to the power-law index of the size distribution by  $q = 5\alpha + 1$ . Assuming that the latitude distribution of scattered KBOs is a Gaussian with a standard deviation  $\sigma_\beta$ , and that a fraction  $f_{\text{SK}}$  of KBOs detected near the ecliptic plane are scattered KBOs,

$$\tau \sim f_{\text{SK}} \pi \theta_{23}^2 \Sigma_{23} e^{\frac{-\beta^2}{2\sigma_\beta^2}} \int dm_R 10^{(\alpha-0.4)(m_R-23)}. \quad (4)$$

Here  $\theta_{23} \equiv r_{23}/a$  is the angular size of a KBO with  $m_R = 23$ .

Assuming that objects at the break magnitude produce occultations above the detection limit, there are two regimes to consider. If the slope of the magnitude distribution above the break magnitude  $m_R > m_b$  ( $r < r_b$ ) is  $\alpha_2 \lesssim 0.4$ , then the integral in equation (4) is dominated by objects near  $m_b$ , and is  $\sim \Delta m_R 10^{(\alpha-0.4)(m_b-23)}$ , where  $\Delta m_R \simeq 0.6|\alpha - 0.4|^{-1} \simeq 3$  is roughly the full-width half-max of the distribution. In the other regime, if  $\alpha_2 \geq 0.4$ , then the integral in equation (4) formally diverges. In practice, the lower limit in radius, or upper limit in magnitude,  $m_{\text{max}}$ , will then be set by where the occultation is too brief or too shallow to be detectable. As I demonstrate in §3, the former generally turns out to be satisfied first. In this regime, the integral in equation (4) is dominated by objects with  $m_R \sim m_{\text{max}}$ , and thus is  $\sim \Delta m_R 10^{(\alpha-\alpha_2)(m_b-23) + (\alpha_2-0.4)(m_{\text{max}}-23)}$ .

A simple boxcar occultation of duration  $2t_c$  has a signal-to-noise  $Q$  of,

$$Q = 2 \langle t_c \rangle \gamma^{1/2} t_{\text{exp}}^{-1/2}, \quad (5)$$

where  $\gamma = 2.46 \times 10^5 \text{ s}^{-1}$  is the rate at which photons will be collected by *Kepler* from a star with  $m_* = 12$ . This expression holds when the occultation duration is less than

the exposure time. For circular KBOs and equatorial occultations, the duration is simply  $t_c = \theta_K/\mu$ , where  $\theta_K$  is the angular radius of the KBO,  $\mu = v/a$  is the proper motion of the KBO, and  $v \sim v_\oplus = 30 \text{ km s}^{-1}$  is the relative velocity of the KBO, which is primarily due to the reflex motion of the Earth. This yields  $t_c \simeq 4 \text{ s } 10^{-0.2(m_R-23)}$ . For objects near the break of  $m_b = 26$ ,  $t_c \simeq 1 \text{ s}$ , and for the planned *Kepler* exposure time of  $t_{\text{exp}} = 15 \text{ min}$ , a typical target star with apparent magnitude  $m_* = 14$  yields  $Q \sim 13$ . The minimum acceptable signal-to-noise of  $Q \sim 7$  (justified in §3) is reached at  $m_{\text{max}} \simeq 27.4$ , where  $r \simeq 16 \text{ km}$ , and  $t_c \simeq 0.5 \text{ s}$ .

Adopting fiducial values for the various input parameters, I now estimate the optical depth in the two regimes. Surveys of bright KBOs find  $\alpha \simeq 0.6$  and  $\Sigma_{23} \sim 1 \text{ deg}^{-1} \text{ mag}^{-1}$  (e.g., Luu & Jewitt 2002). The properties of the scattered KBO population are poorly known due to severe selection biases, and estimates of these properties should therefore be taken with caution. I adopt  $\sigma_i = 20^\circ$  (Brown 2001, hereafter B01; Trujillo, Jewitt & Luu 2001),  $f_{\text{SK}} \sim 0.1$ , and a common distance of  $a = 42 \text{ AU}$ . Assuming a 4% albedo, this yields  $r_{23} \simeq 123 \text{ km}$ , and  $\theta_{23} \simeq 4 \text{ mas}$ . For classical KBOs, the break radius is expected to occur near  $m_b \sim 24$  (Pan & Sari 2004), as is observed (B04). However, scattered KBOs may have longer collision times, and thus the break radius may be smaller. I adopt  $m_b \simeq 26$ , as B04 find for their ‘excited’ subsample. Finally, the FOV of *Kepler* is at  $\beta \simeq 55^\circ$ . Altogether, this yields  $\tau_{\text{br}} \sim 10^{-13}$  for the break-limited regime, and  $\tau_{\text{sn}} \sim 3 \times 10^{-13} 10^{1.4\alpha_2}$  for the signal-to-noise limited regime.

The event rate  $\Gamma$  is related to the optical depth by,

$$\Gamma = \frac{2\tau}{\pi \langle t_c \rangle}, \quad (6)$$

where  $\langle t_c \rangle$  is the mean time scale of the occultation events. Assuming that  $\langle t_c \rangle$  is equal to the time scale at the peak of the size distribution, this yields  $\Gamma_{\text{br}} \simeq 2 \times 10^{-6} \text{ yr}^{-1}$  for the break-limited regime, and  $\Gamma_{\text{sn}} \simeq 10^{-6} \text{ yr}^{-1} 10^{1.4\alpha_2}$  for the signal-to-noise limited regime.

*Kepler* will have  $N_* \sim 10^5$  main-sequence stars in its field-of-view, and will have a lifetime of  $T = 4$  years, so the number of expected events is  $N_{\text{det}} = N_* \Gamma_{\text{br}} T \simeq 0.8$  for the break-limited regime. For the signal-to-noise limited regime, and a faint-end slope of  $\alpha_2 = 0.6$ ,  $\Gamma_{\text{sn}} \simeq 7.7 \times 10^{-6} \text{ yr}^{-1}$ , and the number of expected events is  $N_{\text{det}} = N_* \Gamma_{\text{sn}} T \simeq 3$ .

## 3. EVALUATION OF EVENT RATE

I now provide a somewhat more accurate estimation of the occultation rate in *Kepler's* FOV, taking into account the distribution of KBO radii, inclinations, and velocities; the number, magnitude, and angular size distribution of the target stars; and the suppression of signal-to-noise in occultation events due to diffraction and finite source size effects. Readers who are not interested in these details can skip to §4 without significant loss of continuity. I will continue to make a number of simplifying assumptions, including that all KBOs are located at the same distance of  $a = 42 \text{ AU}$ .

The observable optical depth to a star of a given magnitude  $m_*$  and angular size  $\theta_*$  is

$$\tau(m_*, \theta_*) = \int dm_R \Sigma(\beta, m_R) \Omega(m_R) \Theta(Q - Q_{\text{min}}), \quad (7)$$

where  $\beta$  is the ecliptic latitude of the FOV,  $Q_{\min}$  is the minimum detectable signal-to-noise, and  $\Theta(x)$  is the Heaviside step function.

The surface density  $\Sigma(\beta, m_R)$  of KBOs of a given  $m_R$  at an ecliptic latitude  $\beta$  can be written as,  $\Sigma(\beta, m_R) = \Sigma(0, m_R) f_{\Sigma}(\beta)$ , where  $f_{\Sigma}(\beta)$  is the surface density distribution of KBOs normalized to the ecliptic plane. For a population with an observed inclination distribution at the ecliptic plane of  $f_e(i)$ , this is given by (B01),

$$f_{\Sigma}(\beta) = \int_{\beta}^{\pi/2} di \frac{f_e(i) \sin i}{(\sin^2 i - \sin^2 \beta)^{1/2}} \times \left[ \int_0^{\pi/2} di f_e(i) \right]^{-1}. \quad (8)$$

An inclination distribution of the form  $f_e(i) = \exp(-i^2/2\sigma_i^2)$ , with a standard deviation  $\sigma_i = 20^\circ \pm 4^\circ$ , provides a reasonable fit to the observed distribution of scattered KBOs (B01; Millis et al. 2002; Trujillo, Jewitt & Luu 2001). For this form, the denominator of equation (8) is equal to  $(\pi/2)^{1/2} \sigma_i \text{Erf}(\pi/2\sqrt{2}\sigma_i)$ . The *Kepler* FOV extends over  $10^\circ$  in ecliptic latitude. Since the surface density varies by a factor of  $\sim 2$  over this range for reasonable values of  $\sigma_i$ , I average  $f_{\Sigma}(\beta)$  over  $50^\circ \leq \beta \leq 60^\circ$ , assuming a uniform distribution in  $\beta$ .

For unresolved events ( $2t_c \leq t_{\text{exp}}$ ), I write the signal-to-noise  $Q$  of an occultation as,

$$Q = 2t_c \gamma^{1/2} t_{\text{exp}}^{-1/2} f_{u_0} f_Q 10^{-0.2(m_* - 12)}, \quad (9)$$

whereas, for resolved events ( $2t_c \geq t_{\text{exp}}$ ),

$$Q = (2t_c \gamma)^{1/2} f_{u_0} f_Q 10^{-0.2(m_* - 12)}, \quad (10)$$

Where, as before,  $t_{\text{exp}}$  is the exposure time and  $\gamma$  is the photon collection rate at  $m_* = 12$ . The term  $f_{u_0}$  is the reduction in signal-to-noise due to non-equatorial occultations, which is  $f_{u_0} = \int_0^1 du_0 (1 - u_0^2)^{1/2} = 0.79$  for unresolved events, and  $f_{u_0} = \int_0^1 du_0 (1 - u_0^2)^{1/4} = 0.87$  for resolved events.

Significant suppression of the signal-to-noise due to diffraction and finite-source effects is expected whenever the angular radius  $\theta_K$  of the KBO is comparable to, or smaller than, either the angular size of the star  $\theta_*$ , or the Fresnel angle  $\theta_F = \sqrt{\lambda/2\pi a}$ , where  $\lambda$  is the wavelength of observations. I determine  $f_Q$  by numerically calculating occultation light curves for various values of  $\rho_F \equiv \theta_F/\theta_K$  and  $\rho_* \equiv \theta_*/\theta_K$ , integrating over a bandpass centered at  $\lambda = 500$  nm with a full width of 25%. I then determine the suppression in signal-to-noise of these curves relative to a boxcar complete occultation with duration  $2t_c$ . For unresolved events, for which diffraction and finite-source effects may be important, this can be approximated as

$$f_Q = \frac{1}{4} \text{Erfc} \left( \frac{\log \rho_* - 0.52}{0.42} \right) \text{Erfc} \left( \frac{\log \rho_F}{0.65} \right). \quad (11)$$

For a mid-F dwarf at  $\sim 1$  kpc (typical of Kepler target stars),  $\theta_* \simeq 6 \mu\text{as}$ , while for  $\lambda = 500$  nm and  $a = 42$  AU,  $\theta_F \simeq 23 \mu\text{as}$ . Therefore the diffraction effects are typically expected to be more important than the finite size of the stars. The radius where  $\theta_K = \theta_F$  is  $r \sim 1$  km, or  $m_R \sim 34$ ; the radius where  $\theta_K = \theta_*$  for the example above is  $r \sim 0.26$  km, or  $m_R \sim 37$ . As both of these magnitudes are considerably fainter than the expected cutoff in  $Q$  due to photon noise for the nominal *Kepler* exposure

time, the corrections due to diffraction and finite source effects are small in this case.

The final ingredient in calculating  $Q$  is the radius crossing time  $t_c$ . I determine the relative velocity  $v$  of a KBO at a given ecliptic longitude and latitude by  $v = |\mathbf{v}_{\perp, \oplus} - \mathbf{v}_K|$ , where  $\mathbf{v}_{\perp, \oplus} = \mathbf{v}_{\oplus} - (\mathbf{v}_{\oplus} \cdot \hat{\mathbf{n}})\hat{\mathbf{n}}$ ,  $\hat{\mathbf{n}}$  is the unit line-of-sight vector to the KBO, and  $v_K \equiv v_{\oplus}(a/\text{AU})^{-1/2}$ . I assume circular orbits for the Earth and KBO, and that the KBO is observed at a latitude equal to its inclination. I then average the proper motion  $\mu = v/a$  over ecliptic longitude. This yields  $\langle \mu \rangle = 3.19'' \text{ hr}^{-1}$ , and  $t_c = 3.70$  s for  $r = 100$  km.

The average radius crossing time  $\langle t_c \rangle$  is given by,

$$\langle t_c(m_*, \theta_*) \rangle = \int dm_R \Sigma(\beta, m_R) \frac{\theta_K(m_R)}{\langle \mu \rangle} \Theta(Q - Q_{\min}) \times \left[ \int dm_R \Sigma(\beta, m_R) \Theta(Q - Q_{\min}) \right]^{-1}. \quad (12)$$

This can be combined with the optical depth  $\tau(m_*, \theta_*)$  to yield the event rate,

$$\Gamma(m_*, \theta_*) = \frac{2\tau(m_*, \theta_*)}{\pi \langle t_c(m_*, \theta_*) \rangle}. \quad (13)$$

Finally, the total number of detected occultations can be found by integrating over the magnitude distribution  $dN_*/dm_*$  and angular size distribution  $dN_*/d\theta_*$  of the stars in *Kepler*'s FOV,

$$N_{\text{det}} = T \int dm_* \frac{dN_*}{dm_*} \int d\theta_* \frac{dN_*}{d\theta_*} \Gamma(m_*, \theta_*). \quad (14)$$

I adopt the joint apparent magnitude – spectral type distribution derived by Jenkins & Doyle (2003) and presented in their Table 1; this distribution is in turn based on the Besançon Galactic model (Robin, Reylé, Derrière, & Picaud 2003), assuming an extinction of  $1 \text{ mag kpc}^{-1}$ . Adopting the relations between absolute magnitude, physical radii, and spectral type for main-sequence stars from Allen (1976), the corresponding distribution of angular radii can also be derived.

For the KBO magnitude distribution  $\Sigma(0, m_R)$  near the ecliptic plane, I use the results from B04. They compile data from several surveys, including their own HST results, and fit the surface density distribution to a double power-law form,

$$\Sigma(m_R) = (1+c) \Sigma_{23} \left[ 10^{-\alpha_1(m_R-23)} + c 10^{-\alpha_2(m_R-23)} \right]^{-1}, \quad (15)$$

where  $c \equiv 10^{(\alpha_1 - \alpha_2)(m_b - 23)}$ . For their ‘excited’ subsample, which has  $i > 5^\circ$ , and  $d < 28\text{AU}$  or  $d > 55\text{AU}$ , they find  $\alpha_1 = 0.66$ ,  $m_b = 26.0$ , and  $\Sigma_{23} = 0.39 \text{ mag}^{-1} \text{ deg}^{-2}$ . I estimate that  $\sim 1/3$  of these are scattered KBOs based on the relative number of scattered to resonant KBOs in the B01 analysis. The faint-end slope  $\alpha_2$  is poorly constrained for this sample, but is bounded at 68% c.l. by  $\alpha_2 \lesssim 0.1$  and 95% c.l. by  $\alpha_2 < 0.4$ .

To calculate the rate of detected events, I adopt a signal-to-noise threshold of  $Q_{\min} = 7$ . The total number of flux measurements made by *Kepler* over its lifetime will be  $\sim N_* T t_{\text{exp}}^{-1} \sim 4 \times 10^9$ , therefore requiring a false alarm probability of  $\lesssim 10^{-10}$ . One expects  $\lesssim 1$

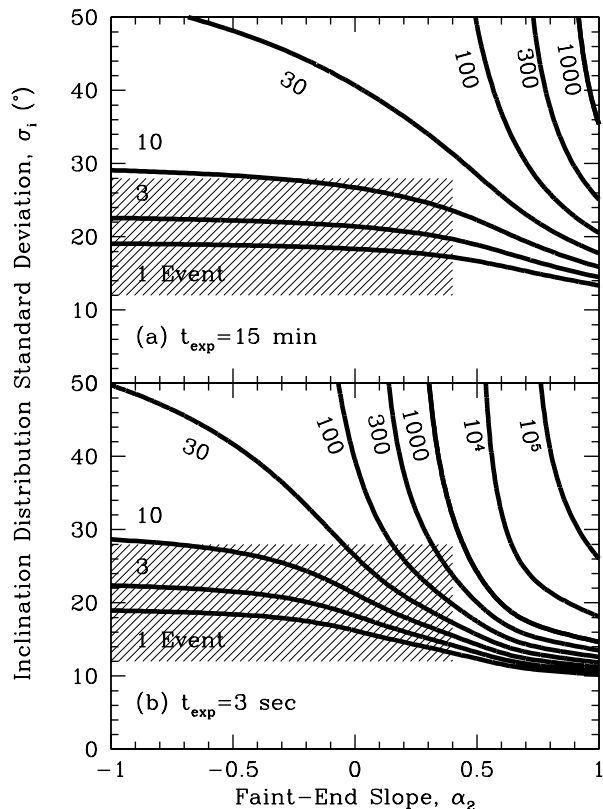


FIG. 1.— The contours show the number of expected occultation events with signal-to-noise  $> 7$  in *Kepler*'s field-of-view, as a function of the standard deviation  $\sigma_i$  of the inclination distribution in degrees, and the faint-end slope  $\alpha_2$  of the surface density versus magnitude relation. The shaded region shows the approximate 95% confidence limits on these parameters. Each panel shows the number of events for a different exposure time. (a) Nominal *Kepler* exposure time of  $t_{\text{exp}} = 15 \text{ min}$ . (b) Exposure time equal to the readout time of 3 seconds.

false alarm for  $Q > 7$ . At the break magnitude  $m_{\text{eq}}$ , the signal-to-noise is  $Q \gtrsim 10$  for  $t_{\text{exp}} = 15 \text{ min}$ . Therefore, the results are not sensitive to the choice of  $Q_{\text{min}}$  for  $Q_{\text{min}} \lesssim 10$ , as long as objects near the break magnitude dominate the integral of the magnitude distribution, i.e. as long as  $\alpha_2 \lesssim 0.4$ .

Figure 1(a) shows number of detected occultation events in *Kepler*'s FOV, as a function of the dispersion in the inclination distribution  $\sigma_i$ , and the faint-end slope  $\alpha_2$ . The change in the shape of the contours near  $\alpha_2 \sim 0.4$  is due to the transition from the break limited to signal-to-noise limited regimes described in the previous section. For  $\alpha_2 \lesssim 0.4$ , the event rate depends mainly on  $\sigma_i$ , whereas for  $\alpha_2 \gtrsim 0.4$ , it depends primarily on  $\alpha_2$ . Very few events are expected for  $\sigma_i \lesssim 10^\circ$  regardless of  $\alpha_2$ . This is due to the exponential suppression of the number of KBOs in the *Kepler* FOV for the assumed Gaussian distribution of inclinations. For the fiducial value of  $\sigma_i = 20^\circ$ , and  $-1.0 \lesssim \alpha_2 \lesssim 0.2$ , the number of events is  $\sim 2$ . This is a factor of a few larger than the rough estimate in the previous section for the break-dominated regime. This difference can be attributed to differences in the assumed number of target stars, surface

density at the ecliptic, and suppression at the latitude of the *Kepler* FOV. The event rate increases steeply for increasing  $\alpha_2 \gtrsim 0.4$ . For  $\alpha_2 = 0.6$ ,  $N_{\text{det}} \simeq 8 \text{ yr}^{-1}$ , again a factor of a few larger than the rough estimate.

#### 4. DISCUSSION

The shaded area in Figure 1 shows roughly the 95% confidence limit on the standard deviation  $\sigma_i$  of the inclination distribution from B01, and the faint-end slope  $\alpha_2$  from B04. In this region, the predicted number of events varies from  $\ll 1$  to nearly 20. Marginalizing  $N_{\text{det}}$  over  $\sigma_i$  and  $\alpha_2$ , assuming Gaussian uncertainty distributions in both parameters with mean and dispersion of  $20^\circ$  and  $4^\circ$  for  $\sigma_i$ , and  $-0.5$  and  $0.6$  for  $\alpha_2$ , yields a best estimate of the number of expected events of  $\langle N_{\text{det}} \rangle \sim 3$ . If no events are detected during the mission lifetime, a 95% confidence upper limit can be placed that should correspond to the  $N_{\text{det}} = 3$  contour, which would exclude roughly half the currently allowed region of  $\sigma_i$  and  $\alpha_2$ .

Although the expected number of events in the 95% c.l. region of  $\sigma_i$  and  $\alpha_2$  is relatively small, it is important to keep in mind that these parameters might be considerably in error, as all previous surveys have had relatively strong selection biases against scattered KBOs. In particular, the constraint on  $\alpha_2$  from B04 is applicable to their 'excited' sample, the majority of which are probably resonant KBOs. Therefore, the faint-end slope of scattered KBOs may differ considerably from that measured by B04; this might even be expected if scattered KBOs were excited early in the formation of the solar system. For  $\alpha_2 \gtrsim 0.4$ , the number of expected events can be quite substantial. In addition to uncertainties in the properties of the known scattered KBO population, there may be additional populations of KBOs at larger distances that are currently undetectable, but may be detected or constrained by *Kepler*.

For unresolved events, the signal-to-noise of occultations scales as  $t_{\text{exp}}^{-1/2}$ . Therefore, the signal-to-noise of individual events can be increased by simply decreasing the *Kepler* exposure time. In the break-limited regime ( $\alpha_2 \lesssim 0.4$ ), where small objects with  $m_R > m_b$  do not contribute much to the optical depth, this does not significantly increase the number of detectable events, although it does improve the reliability of already detectable occultations with  $m_R \lesssim m_b$ . In the signal-to-noise limited regime  $\alpha_2 \gtrsim 0.4$ , decreasing the exposure time can increase the number of detectable occultations dramatically. As currently planned, *Kepler* will only transmit integrations of  $t_{\text{exp}} = 15 \text{ min}$ , due primarily to bandwidth limitations. However, the detectors will in fact be read out every 3 seconds in order to avoid saturation by bright stars. These 3 sec readouts will then be filtered and combined into 15 min integrations. It may be possible, using in-flight software, to search for occultations in the individual 3 sec exposures, and flag and transmit significant events. With this possibility in mind, in Figure 1(b) I show  $N_{\text{det}}$  as a function of  $\sigma_i$  and  $\alpha_2$  for  $t_{\text{exp}} = 3 \text{ sec}$ . As expected, deep in the break-limited regime ( $\alpha_2 \lesssim 0$ ), the number of detectable occultations is similar for  $t_{\text{exp}} = 3 \text{ sec}$  and  $t_{\text{exp}} = 15 \text{ min}$ . However, for  $\alpha_2 \gtrsim 0$ , the number of expected event increases significantly for  $t_{\text{exp}} = 3 \text{ sec}$ . In the allowed region of parameter space, the number of events can be as

large as  $N_{\text{det}} \sim 600$ . Marginalizing over  $\sigma_i$  and  $\alpha_2$  yields  $\langle N_{\text{det}} \rangle \sim 12$ . For  $\alpha_2 = 0.6$ , and  $\sigma_i = 20^\circ$ ,  $N_{\text{det}} \simeq 10^3$ . Whether or not it is efficient or feasible to search the individual 3 sec integrations for occultations remains to be seen. However, given the large potential increase in the number of expected events, and the fact that the subsequent constraints will be hard to acquire with other methods, the possibility should be considered.

Given the fact that the occultation events are unresolved, and have a small amplitude, systematic effects that could mimic occultation events are a serious concern. For a large sample of candidate events, there are some signatures that may differentiate between real occultations and systematics. Occultation events should show a factor of  $\sim 2$  gradient in the optical depth over the  $\sim 10^\circ$  in ecliptic latitude spanned by the *Kepler* FOV. In addition, the relative velocity also varies over the course of the year; for the latitude of the *Kepler* FOV, this variation is  $10 \text{ km s}^{-1}$  peak-to-peak, which corresponds to a variation in both the signal-to-noise and event rate of amplitude  $\sim 30\%$ . Unfortunately, given the intrinsic velocity dispersion of KBOs, and the variation in signal-to-noise due to non-equatorial occultations, it will be difficult to measure these deviations unless there are a large number of events. For individual events, it may be possible to distinguish between occultations and systematic effects based on the detailed shape and centroid of the stellar point-spread function for high signal-to-noise events (Jenkins & Doyle 2003). Ground-based follow-up observations can be used to eliminate contamination from background stars that happen to be blended with the primary star.

It may also be possible to directly detect the KBOs

causing occultation events by imaging them in reflected light. Provided that the data are analyzed in real time, candidate occultation events could be alerted within a day of the event. The signal-to-noise of the occultations should be correlated with their size (e.g., Eq. 9), and therefore brighter events can be preferentially selected for follow-up. The brighter candidates will have  $m_R \sim m_B \simeq 26$  mag, within the range of large, ground-based telescopes. Typical proper motions are a few arcseconds per hour. Therefore, deep imaging taken at several epochs over a few days after the occultation should reveal a faint object moving away from the bright target star.

Provided that systematic effects can be controlled, and a reliable sample of occultation events can be acquired, then the observed distribution of signal amplitudes can be used to statistically infer the distribution of event time scales. This can then be converted to an estimate of the optical depth. If no events are detected, then it should be possible to place limits on the surface density of KBOs in the *Kepler* FOV. Therefore, *Kepler* should measure or significantly constrain the number of highly-inclined,  $\sim 10$  km-sized KBOs.

I would like to thank Josh Bloom, Dave Latham, and Josh Winn for useful discussions, Matt Holman for discussions and reading the manuscript, the anonymous referee for helpful comments and suggestions, and Cheongho Han for the use of his code to calculate occultation light curves. This work was supported by a Menzel Fellowship from the Harvard College Observatory.

#### REFERENCES

- Allen, C. W. 1976, *Astrophysical Quantities* (London: Athlone)
- Bailey, M. 1976, *Nature*, 259, 290
- Bernstein, G. M., Trilling, D. E., Allen, R. L., Brown, M. E., Holman, M., Malhotra, R. 2004, *ApJ*, submitted (astro-ph/0308467) (B04)
- Brown, M. J. I., Webster, R. L. 1997, *MNRAS*, 289, 783
- Brown, M. E. 2001, *AJ*, 121, 2804 (B01)
- Cooray, A. & Farmer, A. J. 2003, *ApJ*, 587, L125
- Dyson, F. J. 1992, *QJRAS*, 33, 45
- Jenkins, J. M., Doyle, L. R. 2003, *ApJ*, 595, 429
- Kaiser, N. et al. 2002, *Proc. SPIE*, 4836, 154
- Liang, C.-L., Rice, J. A., de Pater, I., Alcock, C., Axelrod, T., Wang, A., & Marshall, S. 2003 (astro-ph/0209509)
- Luu, J. X., & Jewitt, D. C. 2002, *ARA&A*, 40, 63
- Malhotra, R. 1995, *AJ*, 110, 420
- Millis, R. L., Buie, M. W., Wasserman, L. H., Elliot, J. L., Kern, S. D., & Wagner, R. M. 2002, *AJ*, 123, 2083
- Millis, R. L., Dunham, E. W., & Sebring, T. A. 2003, *BAAS*, 203, 38.16
- Pan, M., & Sari, R. *Icarus*, submitted (astro-ph/0402138)
- Robin, A. C., Reylé, C., Derrière, S., & Picaud, S. 2003, *A&A*, 409, 523
- Roques, F., Moncuquet, M., Sicardy, B. 1987, *AJ*, 93, 1549
- Roques, F., Moncuquet, M. 2000, *Icarus*, 147, 530
- Roques, F., Moncuquet, M., Lavillonnière, N., Auvergne, M., Chevreton, M., Colas, F., & Lecacheux, J. 2003, *ApJ*, 594, L63
- Trujillo, C. A., Jewitt, D. C., & Luu, J. X. 2001, *AJ*, 122, 457
- Tyson, J. A. 2002, *Proc. SPIE*, 4836, 10